remote sensing

MDPI

Article

Hidden Archaeological Remains in Heterogeneous Vegetation: A Crop Marks Study in Fortified Settlements of Northwestern Iberian Peninsula

Simón Peña-Villasenín, Mariluz Gil-Docampo * and Juan Ortiz-Sanz

Agroforestry Engineering Department, Higher Polytechnic School of Engineering, University of Santiago de Compostela, 27002 Lugo, Spain; s.pena.villasenin@usc.es (S.P.-V.); juan.ortiz@usc.es (J.O.-S.)
* Correspondence: ml.gil@usc.es

Abstract: This study evaluates the effectiveness of multispectral imaging via Unmanned Aerial Systems (UAS), in combination with advanced digital image processing techniques, for the detection and mapping of archaeological sites within diverse landscapes. The research focuses on six case studies located in the northwest of the Iberian Peninsula, a region marked by complex vegetation patterns and varying topography. The primary objective is to assess the potential of these non-invasive remote sensing techniques in identifying crop marks associated with buried structures from ancient, fortified settlements. By means of Principal Component Analysis (PCA) and vegetation indices, the study aims to pinpoint areas of interest that may indicate the presence of archaeological features, while effectively distinguishing them from modern disturbances or natural terrain variations. The research encountered several challenges, including seasonal variations in crop conditions and recent land-use changes. The methodology successfully identified distinct archaeological features. In some instances, natural vegetation variability, typically seen as an obstacle, enhanced the visibility of crop marks, aiding in the detection of underlying structures. These results offer a cost-effective and scalable option for preliminary archaeological surveys, particularly in refining survey methodologies and guiding future excavation efforts aimed at uncovering and preserving ancient, fortified settlements in the region.

Keywords: multispectral sensor; archaeological prospection; Unmanned Aerial System (UAS); principal component analysis (PCA)

check for updates

Citation: Peña-Villasenín, S.; Gil-Docampo, M.; Ortiz-Sanz, J. Hidden Archaeological Remains in Heterogeneous Vegetation: A Crop Marks Study in Fortified Settlements of Northwestern Iberian Peninsula. *Remote Sens.* **2024**, *16*, 3923. https://doi.org/10.3390/rs16213923

Academic Editor: Massimiliano Pepe

Received: 11 September 2024
Revised: 15 October 2024
Accepted: 15 October 2024
Published: 22 October 2024

Copyright: © 2024 by the authors. Licensee MDPI, Basel, Switzerland. This article is an open access article distributed under the terms and conditions of the Creative Commons Attribution (CC BY) license (https://creativecommons.org/licenses/by/4.0/).

1. Introduction

The technique known as crop marks photography is a non-invasive and valuable approach for detecting archaeological sites, based on observing anomalies in the vegetation covering these sites. These anomalies, which sometimes reveal the geometry of hidden structures, arise due to the interaction of these structures with the upper soil layers. In the 1920s, O. G. S. Crawford in the UK was a pioneer in establishing a connection between crop growth and underlying archaeological features [1]. Concurrently, S. Neogrády, a World War I aviator and cartographer, documented what he termed "unnatural phenomena", marking a significant advancement in understanding how variations in vegetation can indicate past human activities [2]. The development of aviation and aerial photography during the same decade allowed others researchers such as G.W.G. Allen and A. Poidebard to conduct extensive studies in several countries, popularizing the technique [3,4].

The advancement of digital technology in the 2000s, with the expansion of digital cameras and GPS use, improved efficiency in collecting aerial archaeological data. Rapid georeferencing of images and the capture of information in spectra beyond the visible, such as Near-Infrared (NIR) and Ultraviolet (UV), have opened new possibilities for detecting crop marks [5]. Additionally, the use of hyperspectral sensors has been explored for crop mark prospecting [6].

Crop marks can be influenced by both the reflectance signature of vegetation over buried archaeological remains and by the crop canopy height and micro-relief of the terrain. Unlike canopy height or micro-relief data, which can be obtained using LIDAR sensors or Structure from Motion (SfM) and Multi-View Stereo (MVS) photogrammetry [7], changes in crop health are more detectable through analysis of multispectral or hyperspectral images [8,9]. Numerous studies address advancements in remote sensing platforms and portable sensors for crop mark detection, as well as improvements in software and analytical techniques for processing and interpreting results [10–13]. A multitude of vegetation indices (VIs) have also been used [14,15]. However, most studies on crop marks have been conducted using aerial images captured from manned aircraft or satellites [16]. These technologies have significant limitations, such as limited spatial resolution, slow data acquisition, atmospheric interference, and high operational costs. In response to these challenges, remote sensing using Unmanned Aerial Systems (UAS) has emerged in recent years as a promising alternative [17].

1.1. Multispectral Sensor and UAS for Crop Mark Detection

Archaeologists have widely adopted the use of UAS equipped with optical cameras (visible spectrum) for various archaeological applications, leveraging their ability to capture high-quality aerial images [18–24]. The ongoing advancement in consumer UAS technology and the reduction in costs for specialized sensors have opened the door to new possibilities. In particular, the more affordable access to multispectral sensors has allowed archaeologists to increasingly consider the use of UAS equipped with this technology for detecting crop marks [25]. Miniaturized multispectral sensors on UAS offer spatial resolutions that can reach the centimetre level, allowing for the identification of extremely subtle crop marks, which are often crucial for archaeology. The ability to fly at low altitudes, without being subject to cloud cover limitations, enables the capture of images with very high spatial and temporal resolution, surpassing the capabilities of traditional satellites and aircraft. These advantages, combined with advanced multispectral data processing techniques, enable the detection of a wide range of anomalies that were previously difficult or costly to identify. Factors such as high image resolution, efficient data collection, and increasing economic accessibility have significantly increased the use of multispectral UAS in archaeology [26]. However, the widespread adoption of this technology still faces challenges, mainly related to the complexity of processing multispectral data, which requires specialized software, advanced technical knowledge, and the ability to manage large amounts of data [27,28]. Additionally, variability in vegetation cover in many archaeological sites continues to raise questions about the universal applicability of this technique.

1.2. Influencing Factors

Although referenced studies establish a connection between buried archaeological features and the surface vegetation growing over them, there are numerous variables that can affect the location of crop marks. Firstly, the type of construction significantly influences the detection of buried structures through crop marks. These can result from various underground constructions, both compact structures, such as walls of enclosed areas or buildings, and open constructions, such as pits or trenches. Negative marks are produced by compact structures, which show more dispersed and weaker vegetation, while positive marks are due to pits or trenches, which present denser and more lush vegetation compared to the surrounding areas [2]. In addition to the type of buried monument, other environmental factors, such as soil moisture and temperature conditions, influenced by seasonal climatic variations, affect the visibility of crop marks [29].

For example, droughts caused by dry climates can increase the visibility of these marks, as occurred in England in 1976 [30]. However, excessive rainfall can have the opposite effect, reducing the number of visible marks, as observed in recent studies [4]. Another factor to consider is the type of crop. Research such as that by [31], shows that certain crops, such as barley, wheat, oilseed rape, and alfalfa, are especially relevant for

detecting archaeological features. Other crops, such as maize, peas, and sunflower, can also reveal similar characteristics. These observations are partly explained by planting methods, plant structure, and their ability to withstand drought and rainfall. Although some studies indicate that crop marks can also be observed in grasslands [32], most have been conducted in uniformly cultivated fields [29]. Geological factors can also affect the visibility of crop marks; for example, the presence of subsurface gravel layers makes marks more prominent in sandy soils compared to clay soils. Authors such as [33,34] highlight the high visibility of crop marks in alluvial fans or cones, where soil composition and vegetation dynamics favour the formation of these marks. Other studies have explored the optimal period for detecting crop marks using methodological procedures involving repeated temporal observations [5]. This approach allows determining the most suitable time range for detecting these marks [35]. Previous research has identified that the most favourable period for detection usually falls between mid-April and mid-May [36,37].

However, authors such as [38] note that although many cultivated plant species show anomalies from the early stages of their growth cycle, it is during the maturation process that more significant variations can be detected. However, the methods and conclusions obtained in these studies are mostly applicable to anthropogenic crops and not to natural crops, where growth dynamics and interactions with the environment can differ significantly. It is worth noting that this study was conducted using RGB images only.

Despite the mentioned advancements, detecting buried archaeological remains a complex challenge in studying human history. The success of this task largely depends on the preservation of archaeological remains and their interaction with the surrounding environment. Factors such as the type of structure, environmental conditions, vegetation cover, the time of year, and the characteristics of the platform and sensor used introduce a series of variables that complicate the evaluation of the technique's performance, maintaining a degree of uncertainty in its application. This uncertainty is even greater in environments with natural crops compared to monoculture areas, which have been the focus of existing literature. Although the scientific literature on this topic is extensive, few studies analyse the performance of these techniques in natural crop contexts. This study addresses this gap by investigating the utility of crop marks in heterogeneous archaeological sites, such as fortified settlements in the northwest of the Iberian Peninsula. With 13 multispectral aerial surveys of five settlements, taken at different times between 2021 and 2023, the aim is to analyse how contextual variables influence the detection of crop marks through multispectral remote sensing using UAS.

2. Materials and Methods

The following section describes the case studies, the human and material resources, and the steps for the complete development of the work.

2.1. Case Studies

Figure 1 shows the location of the selected archaeological sites as case studies. In order to conduct the analysis across different contexts, the case selection includes various site types, primarily Bronze Age and Iron Age hillfort settlements, but also Roman or Romanized settlements, as well as a medieval castle.

Sites with no prior excavations, such as the one shown in Figure 2B, and sites with partial excavations, like the one observed in Figure 2A, have been selected. The presence of multiple study areas with distinct characteristics within the sites was also a determining factor, as seen in Figure 2A,B, where differentiated areas of grass versus scrubland are apparent. One of the case studies also includes a site area that has recently experienced a fire, thus broadening the context to include areas with post-fire vegetation regeneration (Figure 2C).

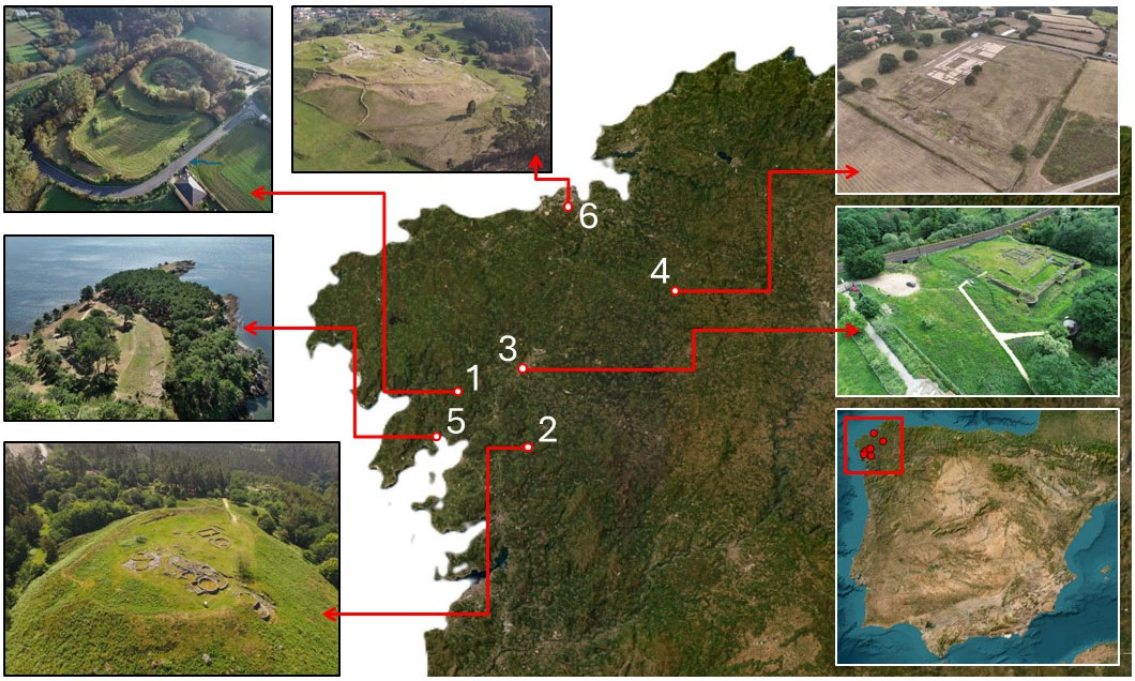


Figure 1. Location of case studies at the Northwest of Spain. Case 1: Castro de Comparada. Case 2: Castrolandín. Case 3: A Rocha Forte Castle. Case 4: Ciudadela de Sobrado dos Monxes. Case 5: Castro Neixón. Case 6: Castro de Elviña.

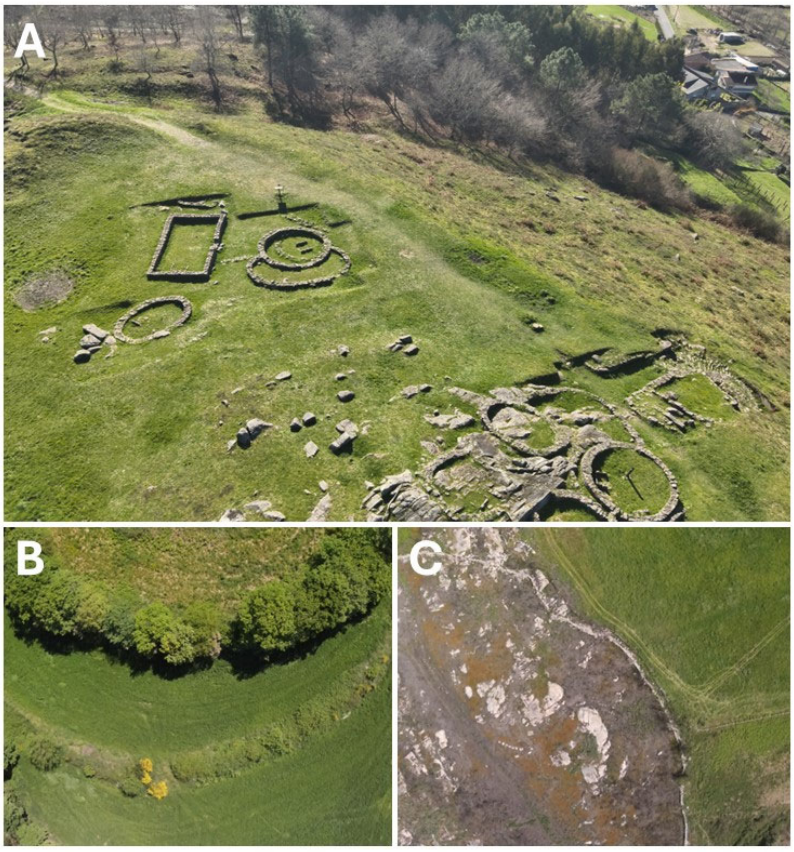


Figure 2. (**A**) Oblique image of Case 2 showing a grassland area on the left and shrubland on the right. (**B**) Vertical photo of Case 1 showing the shrubland area at the top and the grassland area at the bottom. (**C**) Vertical photo of Case 6 showing the area affected by fire on the left part.

2.1.1. Case 1—Castro de Comparada, Lousame

The Castro de Comparada is an Iron Age settlement located in the municipality of Lousame, in the province of A Coruña. This site features typical structures of the castro culture, such as circular dwellings and defensive walls. The choice of this site is due to the fact that the annual agricultural work in the area makes it a favourable environment for detecting crop marks, as most previous studies have shown that cultivated soils are ideal for this technique. It also has a clearly distinct area from the first one with a higher density of shrubland.

2.1.2. Case 2—Castrolandín, Cuntis

Castrolandín, located in the municipality of Cuntis, is an Iron Age site notable for its defensive structures and internal organization. This site undergoes regular maintenance with two annual manual brushings, which promotes the regeneration of pastures. These activities can be beneficial for locating crop marks, as they allow observation of how maintenance work influences the visibility of these marks in a controlled pasture environment. Additionally, as it is partially studied, it allows for the verification of whether visible structures correlate with possible crop marks in the unexcavated areas.

2.1.3. Case 3—Castle of A Rocha Forte, Santiago de Compostela

The Castle of A Rocha Forte, located near Santiago de Compostela, is a medieval site dating back to the 13th century. This castle was a significant fortification during the Middle Ages and features notable defensive structures such as robust walls and moats, which have not been previously excavated. The site's dense and varied vegetation poses challenges for the detection of crop marks. Despite these challenging conditions, the confirmed presence of defensive walls and moats makes this site valuable for studying the effectiveness of crop mark detection techniques. The goal is to evaluate how well these techniques perform under less-than-ideal vegetative conditions and to determine if they can successfully identify features of the castle that are otherwise obscured by vegetation.

2.1.4. Case 4—Roman Camp of A Cidadela, Sobrado dos Monxes

The Roman camp of A Cidadela, located in the municipality of Sobrado dos Monxes, in the province of A Coruña, is an imperial-era site characterized by its regular and symmetrical structure, which includes barracks, roads, and perimeter defenses. This architectural organization facilitates the interpretation of crop marks, as straight lines and geometric patterns are easier to detect and analyze compared to the more organic design of castro sites. The site is regularly maintained, resulting in a pasture surface ideal for analyzing crop marks. The well-defined layout and continuous management of the land provide a favorable context for studying how different types of vegetation and maintenance practices influence the visibility and detection of crop marks.

2.1.5. Case 5—Castro de Neixón, Rianxo

The Castro de Neixón is located in a coastal area in the municipality of Rianxo. This site, dating back to the Bronze and Iron Ages, includes two main areas: Neixón Grande and Neixón Pequeno. Its milder coastal environment, compared to inland sites, may promote more consistent vegetation regeneration, which could enhance the visibility of crop marks throughout the year. This site has been selected to assess how coastal climatic conditions impact the appearance and visibility of crop marks.

2.1.6. Case 6—Castro de Elviña, A Coruña

The Castro de Elviña, located in the city of A Coruña, is one of the most significant archaeological sites in the northwest of the Iberian Peninsula due to its extensive area and historical importance. Dating back to the Iron Age, it features a complex network of walls, dwellings, and other defensive structures. Its large surface area makes it ideal for detecting crop marks, as the extensive space allows for a greater appearance of these marks.

Additionally, the site's archaeological significance adds value to the study of the technique in a context of high importance. The site undergoes regular maintenance, providing an ideal area of pasture for the analysis of crop marks. It also includes an area of scrubland that has recently experienced a fire, allowing for the study of the technique in a post-fire context.

2.2. Material Resources

To assess the performance of the methodology in the case studies, a range of human and material resources were involved. The human resources required include at least one UAS pilot and a technician with expertise in photogrammetry and GIS. This team is responsible for planning and capturing multispectral images with UAS, as well as for photogrammetric processing, orthorectification of images, and the subsequent delineation and interpretation of crop marks. On the material side, the project necessitates UAS for image capture, processing software for handling photogrammetric tasks, and computing hardware capable of managing and processing the collected data.

For capturing multispectral images at the study sites, the DJI Phantom 4 Multispectral UAS was used. This consumer model, introduced in 2019, is well-regarded for its effectiveness in remote sensing applications and is priced around $5000–6000. The Phantom 4 Multispectral is praised for its user-friendly design, being a Ready-to-Fly unit with all integrated systems. It is equipped with six 1/2.9 CMOS sensors, each with a pixel count of 2.08 MP. This includes one optical sensor for the visible spectrum and five monochrome sensors dedicated to multispectral imaging (Blue, Green, Red, Red-Edge, and Near-Infrared). The spectral responses of the multispectral sensor are detailed in Table 1.

Table 1. Spectral responses.

Band	*Central Wavelength (nm)*	*Bandwidth (±nm)*	*Spectral Range (nm)*
Blue	450	±16	434–466
Green	560	±16	544–576
Red	650	±16	634–666
Red-Edge	730	±16	714–746
Near-Infrared	840	±26	814–866

The UAS utilizes Real-Time Kinematic (RTK) positioning systems to ensure accurate location data throughout the flight, providing high-quality georeferenced images. With a flight time of up to 27 min per battery, it allows for extensive coverage in a single flight session, which supports precise detection of vegetation and other terrain details. As the Phantom 4 Multispectral's remote control does not have an integrated screen, flight planning and control are managed using the DJI GS Pro application installed on a 10-inch Apple iPad, as shown in Figure 3B.

In Table 2 the material costs associated with the equipment used for capturing and processing multispectral images are presented.

Table 2. Material Costs.

Equipment	*Launch Price ($)*
UAS DJI PH4 Multispectral	6000
Apple iPad 6th generation	400
DJI GS PRO App 2.0.11	Free
Agisoft Metashape Professional Software 1.7.4 build 12584	4000
QGIS Desktop 3.22.16 Software	Free
Intel(R) Core(TM) i7-7800X CPU + GeForce GTX 960 GPU	2500



Figure 3. Equipament (**A**) Phantom 4 Multispectral (**B**) PH4M sensor (**C**) Flight Planning for Case 6.

2.3. Work Steps

The processing of results is divided into four steps: multispectral photogrammetric registration with UAS, multiband photogrammetric processing, post-processing of orthomosaics, and interpretation and vectorization of crop marks. Each of these steps is detailed below.

2.3.1. Step 1—Multispectral Photogrammetric Registration with UAS

In standard fieldwork for multispectral photogrammetry using UAS, two main tasks are typically carried out: establishing a network of Ground Control Points (GCPs) and executing photographic capture according to a pre-established plan. However, in this study, GCPs were not used since the UAS is equipped with an RTK system that ensures sufficient accuracy in the georeferencing of results. Therefore, the first task was omitted, and the focus was solely on photographic registration.

Using the DJI GS PRO application, flights were planned and executed with the recommended overlaps for photogrammetric reconstruction: 80% longitudinal overlap and 70% transverse overlap [39,40], fully covering the study area. Flights were conducted at an altitude between 45 and 110 m above the ground, resulting in a Ground Sample Distance (GSD) of 3–6 cm. The flight dates were selected based on the availability of human and material resources between 2021 and 2023.

2.3.2. Step 2—Multiband Photogrammetric Processing

The process followed the three main phases of the SfM-MVS pipeline. First, internal and external orientation of the images was performed. Second, a high-density point cloud was generated. Finally, a 3D mesh and a Digital Elevation Model (DEM) were created, enabling ortho-rectification and mosaicking of the images. Since GCPs were not employed,

to improve the precision of the relative alignment of the orthomosaic, the coordinates of significant points from the first flight were extracted and used as reference points for subsequent flights in cases involving multiple flights. This ensured proper alignment of ortho-mosaics from different dates, which is crucial for comparing multitemporal results.

To obtain the actual reflectance values, the images were calibrated using solar sensor data from the tool provided by Metashape for this purpose. Unlike standard RGB photogrammetric processing, generating a multispectral orthomosaic requires exporting a multiband file. After processing the orthomosaic bands, which contained 16-bit integer values, the reflectance was normalised by scaling it to the range of 0 to 1. In this context, 100% reflectance corresponds to the maximum value of 65,535 within the range of 0 to 65,535. To adjust the output bands, the raster calculator was used to divide the original values by 32,768, the middle of the available range [41]. Finally, the orthomosaics were exported as a multiband TIFF file with the bands Blue (1), Green (2), Red (3), Red-Edge (4), and NIR (5). The process for generating the orthomosaic is extensively documented in the existing literature, both for optical images and for multiband orthomosaics [42,43].

2.3.3. Step 3—Post-Processing of Orthomosaics

The post-processing of the orthomosaics was performed using QGIS Desktop 3.22.16 "Białowieża" (Quantum GIS), an open-source software developed by the Open Source Geospatial Foundation (OSGeo), USA, and involved three main types of analysis. First, true-color and false-color composite orthomosaics were generated for each flight using the Red-Green-Blue (RGB) color bands. Second, principal component analysis (PCA) was performed using two plugins: PCA and SCP. This analysis was applied to both individual orthomosaics and combined orthomosaics from different dates, generating five components for individual orthomosaics and ten components for paired mosaics. Various color compositions were created with both, individual and combined PCAs. Finally, using the raster calculator, individual maps based on vegetation indices were created. The complete list of indices tested in this study is shown in Table 3.

Table 3. Formulas of the indices tested.

INDEX	FORMULA
NDVI (NORMALIZED DIFFERENCE VEGETATION INDEX)	$(NIR - Red)/(NIR + Red)$
NDVIRE (NORMALIZED DIFFERENCE VEGETATION INDEX FOR RED-EDGE)	$(NIR - Red\text{-}Edge)/(NIR + Red\text{-}Edge)$
NDRE (NORMALIZED DIFFERENCE RED-EDGE)	$(NIR - Red\text{-}Edge)/(NIR + Red\text{-}Edge)$
SAVI (SOIL ADJUSTED VEGETATION INDEX)	$(NIR - Red)/(NIR + Red + 0.5) \times (1 + 0.5)$
NLI (NONLINEAR VEGETATION INDEX)	$(NIR^2 - Red)/(NIR^2 + Red)$
GEMI (GLOBAL ENVIRONMENT MONITORING INDEX)	$\eta \times (1 - 0.25 \times \eta) - ((Red - 0.125)/(1 - Red))$ $\eta = ((2 \times (NIR^2 - Red^2) + 1.5 \times NIR + 0.5 \times Red)/(NIR + Red + 0.5))$
TVI (TRIANGULAR VEGETATION INDEX)	$0.5 \times (120 \times (NIR - Green) - 200 \times (Red - Green))$
MTVI (MODIFIED TRIANGULAR VEGETATION INDEX)	$1.2 \times (1.2 \times (NIR - Green) - 2.5 \times (Red - Green))$
GDVI (GREENNESS DIFFERENCE VEGETATION INDEX)	$(NIR - Green)/(NIR + Green)$
CHLGREEN (CHLOROPHYLL GREEN)	$(NIR/Green) - 1$
TCARI (TRANSFORMED CHLOROPHYLL ABSORPTION RATIO INDEX)	$3 \times ((Red\text{-}Edge - Red) - 0.2 \times (Red\text{-}Edge - Green)) \times (Red\text{-}Edge/Red)$
MCARI (MODIFIED CHLOROPHYLL ABSORPTION REFLECTANCE INDEX)	$((Red\text{-}Edge - Red) - 0.2 \times (Red\text{-}Edge - Green)) \times (Red\text{-}Edge/Red)$
ARI (ANTHOCYANIN REFLECTANCE INDEX)	$(1/Green) - (1/Red\text{-}Edge)$
NGRDI (NORMALIZED DIFFERENCE GREEN/RED INDEX)	$(Green - Red)/(Green + Red)$

2.3.4. Step 4—Interpretation and Vectorization of Crop Marks

Finally, the vectorization of the crop marks observed in the orthomosaics, and calculated indices was carried out. Due to the high heterogeneity of the study areas, individualized enhancements were applied using contrast stretching in the range of 2% to 98% of the intensity values for each specific area in most cases. This process was performed on all generated information layers, including individual layers and coloured compositions, vectorizing all possible crop marks. In some case studies, the marks were classified into two levels of probability for correspondence with structures, considering geometric arrangement, intensity of the crop marks, their temporal continuity across different flight dates, and their spectral continuity across different information layers. Special attention was given to areas where previous archaeological excavations had been conducted to analyse their correspondence with the detected crop marks. The vectorization was carried out using the free software QGIS. The work was executed by GIS technicians without specialization in archaeological heritage.

3. Results

The following section presents the main results obtained from the six case studies. Table 4 details the outcomes of the recording campaigns, including the characteristics of the study sites. It covers the type of land cover, the extent of each area, the dates when the flights were conducted, the prevailing weather conditions during those times of the year, the average number of multispectral images captured, the flight altitude and GSD for each case.

Table 4. Flight Results.

Case	Type of Land Cover	Site Extent	Dates	Weather	No. Images (5 Bands)	Flight Altitude (m)	GSD (Cm)
Case 1	Grassland and Scrubland	1.5 Ha	May 2022	Mild Spring	89	85	4.4
Case 2	Grassland and Scrubland	1.2 Ha	August 2021 May 2022	Dry Summer Mild Spring	185	70	3.7
Case 3	Grassland	0.7 Ha	August 2021	Dry Summer	321	40	2.1
Case 4	Grassland	2.5 Ha	June 2022 October 2022 March 2023	Mild Spring Dry Autumn Rainy Winter	126	75	3.8
Case 5	Grassland	2 Ha	September 2021 May 2022 September 2022	Dry Summer Mild Spring Dry Summer	437	60	3.5
Case 6	Grassland and Scrubland Affected by Fire	19 Ha	August 2022 February 2023 April 2023	Dry Summer Rainy Winter Rainy Winter	867	110	5.6

3.1. Results of Photogrammetric Processing

As a result of the photogrammetric processing, the internal and external calibration parameters of the cameras were obtained, individually for each band. Calibration reports for the cameras used in the six case studies on the first flight date are available in the Supplementary Materials. The processing parameters for all results can be consulted in these reports. Figure 4 shows the 3D mesh obtained (Figure 4A) and the Digital Elevation Model (Figure 4B). These surfaces enabled the orthorectification of images for creating the multispectral orthomosaic with 5 bands: Blue (1), Green (2), Red (3), Red-Edge (4), and NIR (5). Figure 4C displays the true color composition of the orthomosaic for Case Study 2.

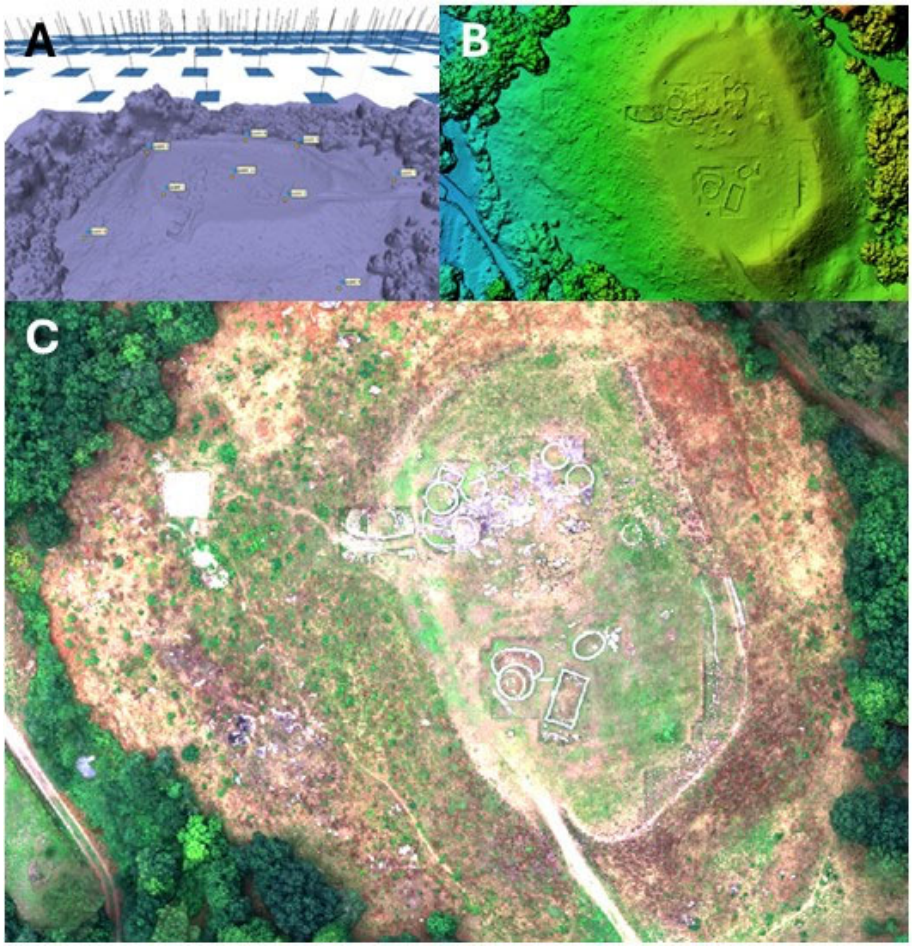


Figure 4. Case 2: (**A**) Triangle mesh, (**B**) Digital Elevation Model (DEM), (**C**) True color orthomosaic (RGB).

3.2. Orthophotos Index and Vectorization Results

The following presents detailed results for each case study, with an emphasis on key findings in the identification of crop marks and their interpretation.

3.2.1. Case 1

In the first case study, a single multispectral flight was conducted. Figure 5A shows the obtained RGB orthophoto. Various anomalies were observed on the surface of the site, suggesting the possible presence of archaeological remains. The initial vectorization of the crop marks on this orthophoto (Figure 5B) provided a vector record, laying the groundwork for detailed analysis. The NDVI index proved to be the most effective for identifying crop marks, as shown in Figure 5C. Vectorization using this index revealed marks that were less evident in the original RGB orthophoto, enhancing clarity and precision in identifying these structures, which are marked in red in the figure. Further analysis with individual bands (Figure 5D) and color compositions (Figure 5E,F) derived from the PCA of the five spectral channels contributed to consolidating the identification of previously detected crop marks and revealed other possible crop marks, vectorized in cyan or yellow in the figures. Although the SAVI and NDRE indices did not surpass the NDVI in effectiveness, the application of PCA significantly enhanced the visualization of these marks, providing greater confidence in the results. The color compositions RGB in Figure 5E,F were created using the first three PC, which allowed for a more distinct and comprehensive representation of the detected features. The arrow indicates the direction of north.

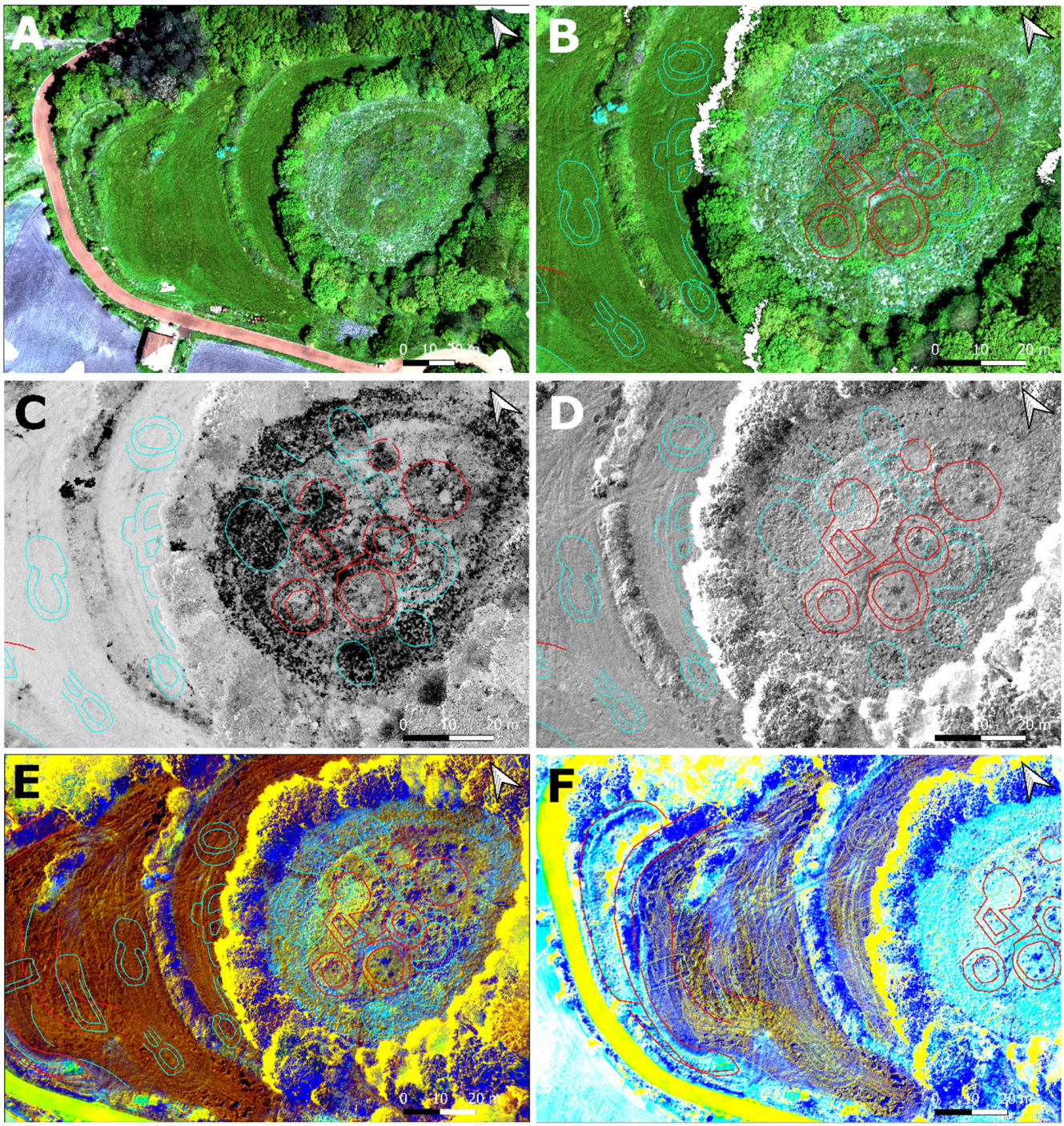


Figure 5. Case 1. (**A**) RGB Orthophoto. (**B**) Crop marks vectorization over RGB Orthophoto. (**C**) NDVI index. (**D**) PCA First component. (**E**) PCA Color Composition for Zone 1. (**F**) PCA Color Composition for Zone 2. The arrow indicates north.

Specific enhancement adjustments were applied to each area of the site using the first three PC, which highlighted areas of particular interest. In Figure 6A, corresponding to a predominantly scrubland area, the adjusted enhancements allowed for clearer identification of crop marks. In contrast, Figure 6B shows a pasture area with specific enhancement adjustments for that zone, where both archaeological crop marks and recent agricultural machinery marks were detected. The latter complicates the interpretation of results, as they can easily be confused with archaeological crop marks.

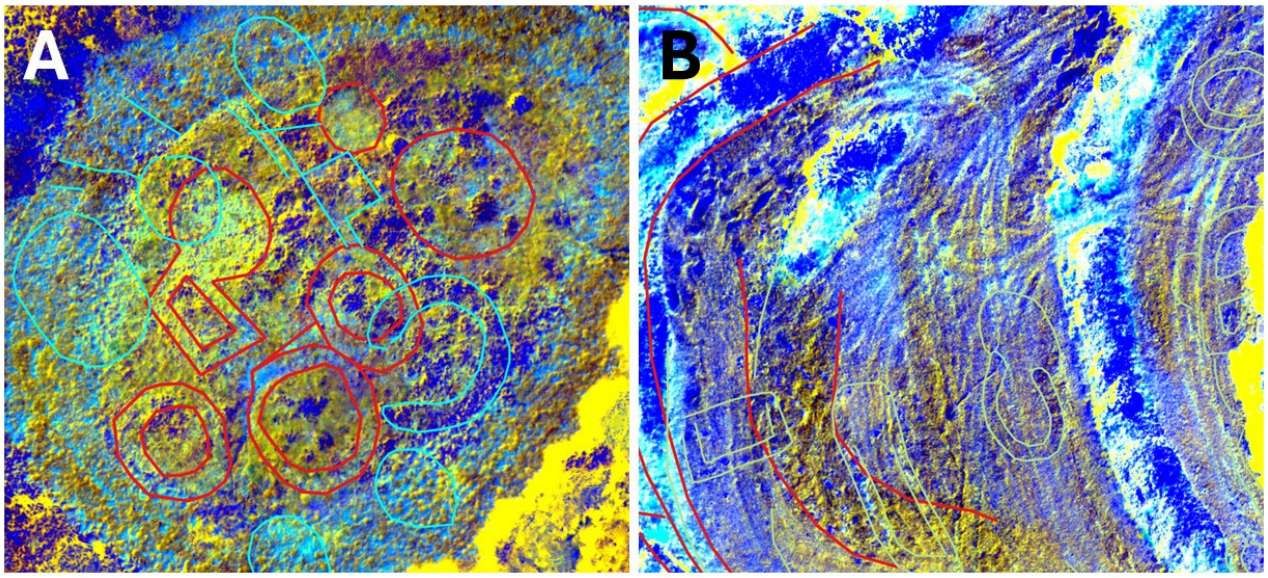


Figure 6. PCA 123 Color Composition. (**A**) Scrubland Zone. (**B**) Pasture Zone.

In conclusion, for the first case study, the image analysis demonstrated that the NDVI index was the most effective for highlighting crop marks. The NDVI index and the use of PCA compositions allowed for better visualization of the marks, especially in Zone 1. However, the presence of machinery marks in Zone 2 underscores the complexity of distinguishing between archaeological crop marks and recent surface disturbances, highlighting the importance of careful analysis to correctly interpret anomalies detected at archaeological sites.

3.2.2. Case 2

In the second case study, two multispectral flights were conducted. The RGB orthophotos obtained (Figure 7A,B), especially from August 2021 (Figure 7A), also show anomalies suggesting the presence of buried structures. Figure 7 shows crop marks vectorized in red using the NDVI index, and in gray using other color compositions. The false-color composition 123 (Figure 7C) is observed to facilitate the identification of crop marks compared to the composition 321 (Figure 7A). The initial vectorization of the crop marks on these orthomosaics is presented both in this false-color composition (Figure 7C) and on the NDVI index from the same flight (Figure 7D). Figure 7E shows the vectorized crop marks over the color composition 123 from the PCA of the spectral bands from the August 2021 and May 2022 flights. Like Case 1, the NDVI index proved to be particularly useful for identifying crop marks, as seen in Figure 7C. This index allowed the detection of marks that were not evident in the RGB orthophoto. Other indices did not provide significant improvements compared to NDVI. The maintenance work involving manual clearing seems to facilitate the detection of these marks at the site. In the shrubland area, some structures were detected that could correspond to circular dwellings, as the dimensions of the excavated houses nearby match the detected marks.

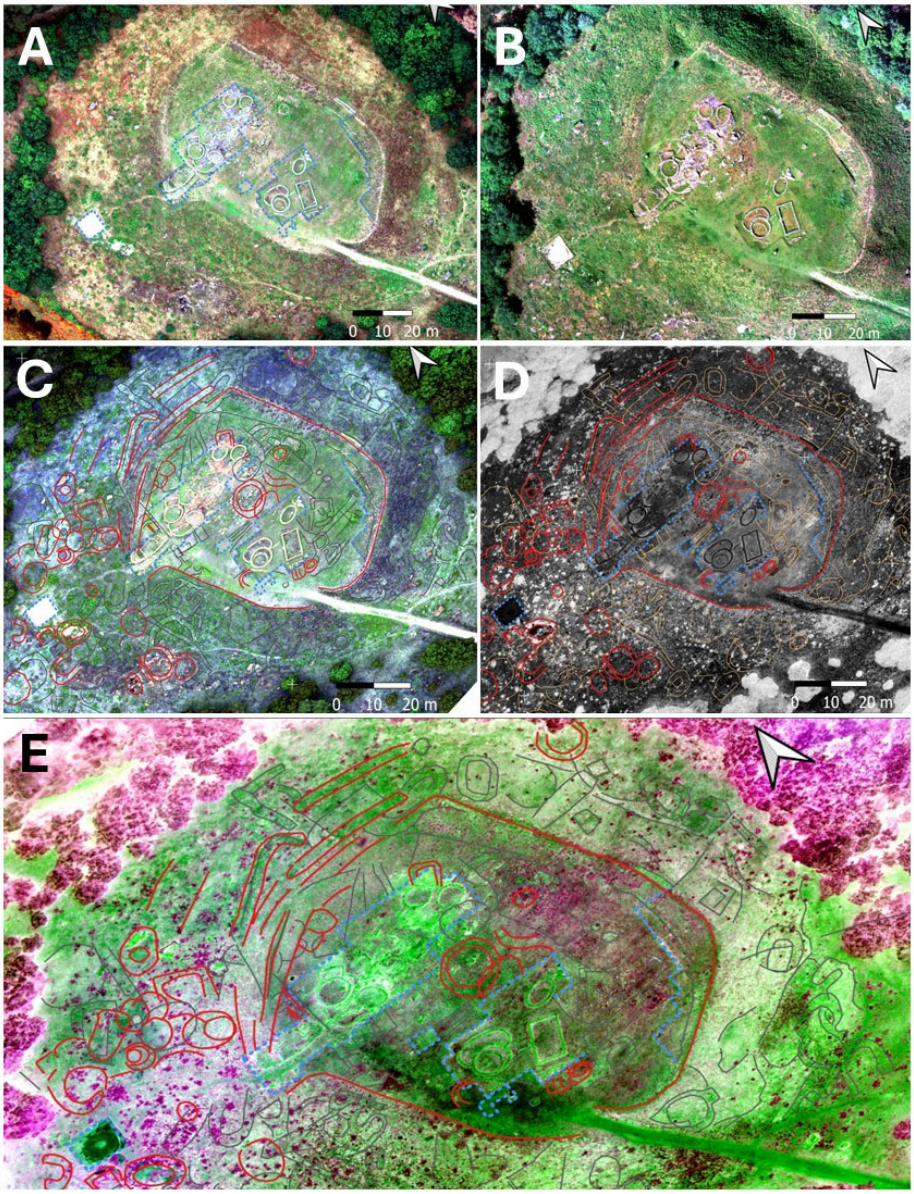


Figure 7. (**A**) True color composition (321) from August 2021. (**B**) True color composition (321) from May 2022. (**C**) Crop marks over the false color composition (123) from August 2021. (**D**) Crop marks over NDVI index from August 2021. (**E**) Crop marks over the combined PCA of both flights, composition 146.

Figure 8 shows a mosaic of coloured compositions, PCA analysis, and vegetation indices of a crop mark clearly related to an archaeological structure buried in the pasture area. This crop mark was clearly identified in the results of the August 2021 flight; however, it was not detectable in the May 2022 flight, highlighting the significant influence of the context on the effectiveness of the technique. The NDVI and SAVI indices proved to be the most effective for detecting the buried structure. These marks are also visible in the false-color compositions from the August 2021 flight, such as composition 325, as well as in various coloured PCA compositions from the combined flights, including the one shown in Figure 8H.

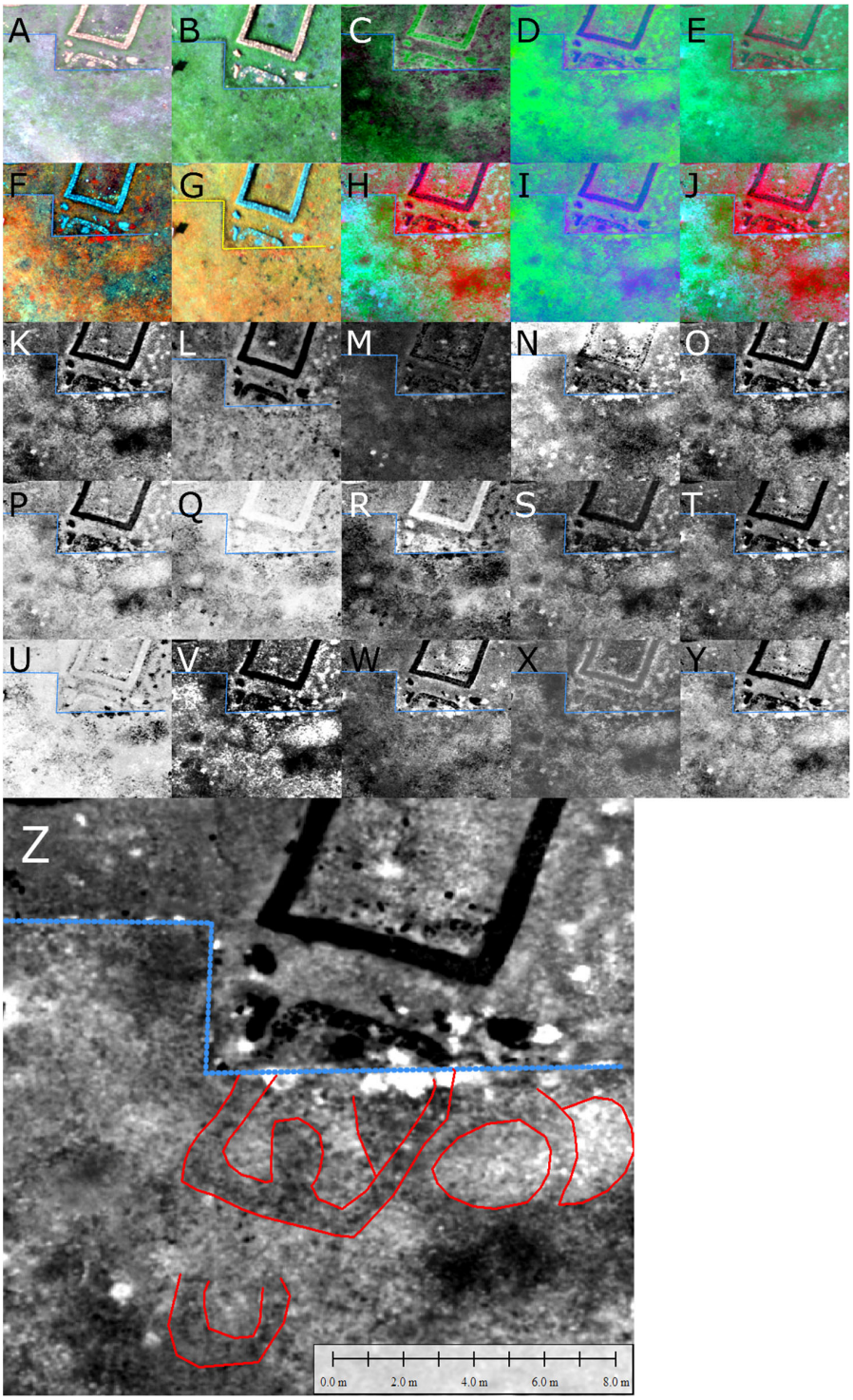


Figure 8. Mosaic of color compositions and indices. (**A**) RGB—August 2021. (**B**) RGB—May 2022. (**C**) PCA August 2021, composition 123. (**D**) PCA August 2021, composition 147. (**E**) PCA August 2021, composition 159. (**F**) Color Infrared August 2021, composition 521. (**G**) Color Infrared May 2022, composition 521. (**H**) Combined PCA, composition 149. (**I**) Combined PCA, composition 147. (**J**) Combined PCA, composition 159. (**K**) NDVI August 2021. (**L**) NDVI May 2022. (**M**) NDVI RE August 2021. (**N**) NDRE August 2021. (**O**) SAVI August 2021. (**P**) NLI August 2021. (**Q**) GEMI August 2021. (**R**) TVI August 2021. (**S**) MTVI August 2021. (**T**) ChiGREEN August 2021. (**U**) TCARI August 2021. (**V**) MCARI August 2021. (**W**) ARI August 2021. (**X**) NGRDI August 2021. (**Y**) GDVI August 2021. (**Z**) Crop marks on NDVI August 2021.

3.2.3. Case 3

In the third case study, a single flight was conducted. Figure 9A shows the obtained RGB orthomosaic. Figure 9B presents the vectorization of the crop marks on this orthomosaic, while Figure 9C illustrates the same crop marks on the NDVI index. The cyan lines indicate the location of the site's outer wall, while the red lines indicate other crop marks detected in the various indices and color compositions.

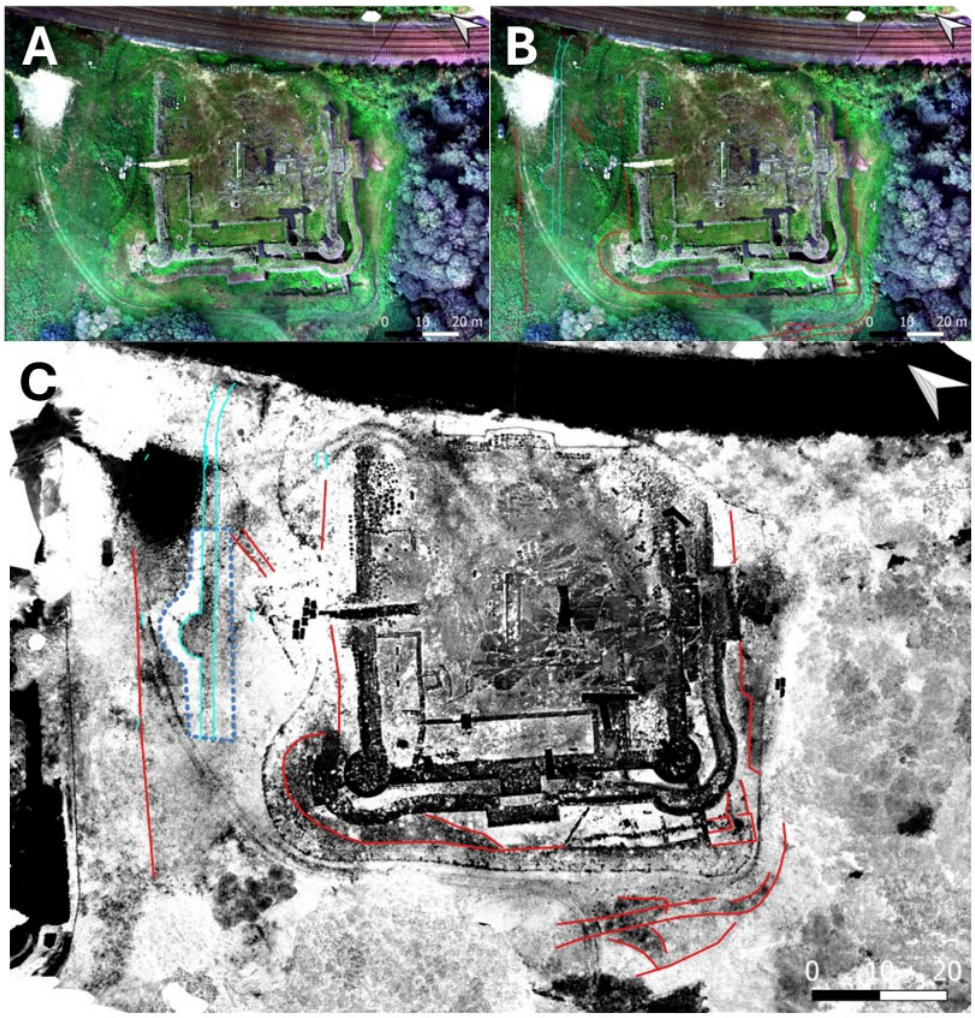


Figure 9. (**A**) True color orthomosaic (RGB). (**B**) Crop marks on RGB orthomosaic. (**C**) Crop marks on NDVI index. The arrow indicates north.

In this case, as seen in Figure 10, the high contrast of the crop mark associated with the remains of the defensive wall, which has been documented since excavations conducted in 2020 at this site, is noteworthy. The crop mark clearly delineates the excavated area (blue dashed line) and the defensive structure. In the area adjacent to the excavated section, subtle crop marks that appear to correlate with the structure suggest that preliminary identification of such elements can be achieved through image analysis. Although vehicle and pedestrian traffic has complicated the interpretation of the crop marks, subtle marks have also been detected at the edge of the moat adjacent to the wall. This supports the hypothesis that such negative structures (positive crop marks) can also be delineated. In other areas of the site, where it is suspected that the wall might extend, clear crop marks have not been identified, though this does not rule out the possible presence of the structure in those locations.

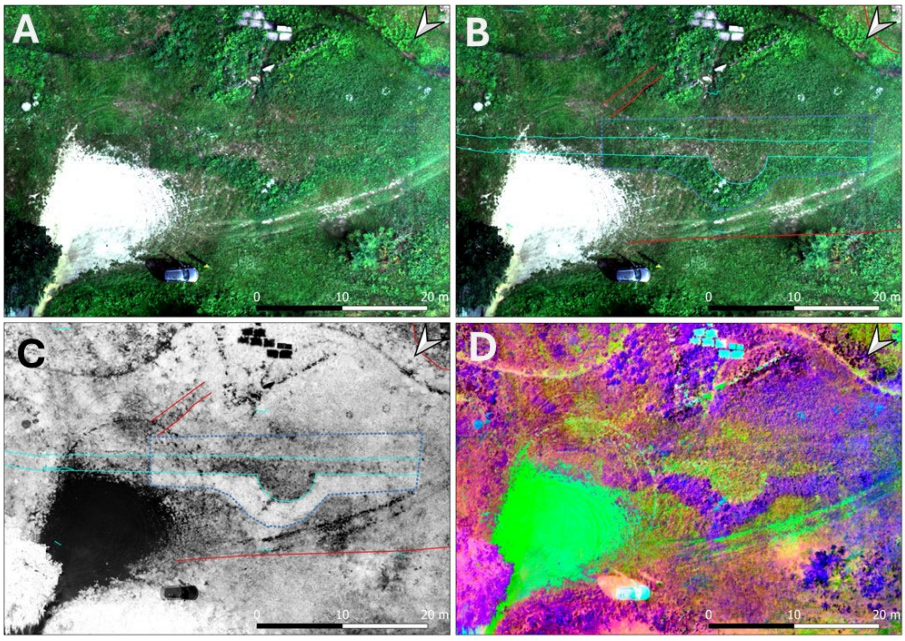


Figure 10. Detail of crop mark in the previously excavated defensive wall area. (**A**) RGB orthomosaic. (**B**) Crop marks over RGB orthomosaic. (**C**) Crop marks over NDVI. (**D**) PCA 123 color composition.

3.2.4. Case 4

In the fourth case study, three multispectral flights were conducted. Figure 11A–C display the true color orthomosaics corresponding to the three dates. Figure 11 presents the crop marks vectorized in red using the NDVI index, and other possible crop marks in cyan, vectorized using color compositions or other indices. Figure 11D presents the vectorized crop marks over the March 2023 orthomosaic. This date, early in spring, provided the best detection of crop marks in this case. The early summer 2022 flight also identified crop marks, but to a lesser extent. The October flight showed too many disturbances due to recent clearing activities at the site during that period.



Figure 11. RGB Orthomosaics: (**A**) June 2022, (**B**) October 2022, (**C**) March 2023. (**D**) Crop marks over March 2023 RGB orthomosaic. The arrow indicates north.

Despite the site being partially excavated, no crop marks were clearly associated with the already-excavated structures. However, crop marks with a higher probability of corresponding to ancient structures or recent human activities were vectorized in red. As in previous cases, most of these crop marks were identified through vegetation indices, especially the NDVI indices (Figure 12A–C) and the PCA 123 color compositions of combined flights (Figure 12D–F). Other, less evident structures were vectorized in cyan. Figure 12G shows the NDVI difference between the last two flight dates, another analytical approach that yielded good results for this case study. This was not the case for the NDVI between the first and second flights, as clearing activities at the site altered the multi-temporal analysis results.

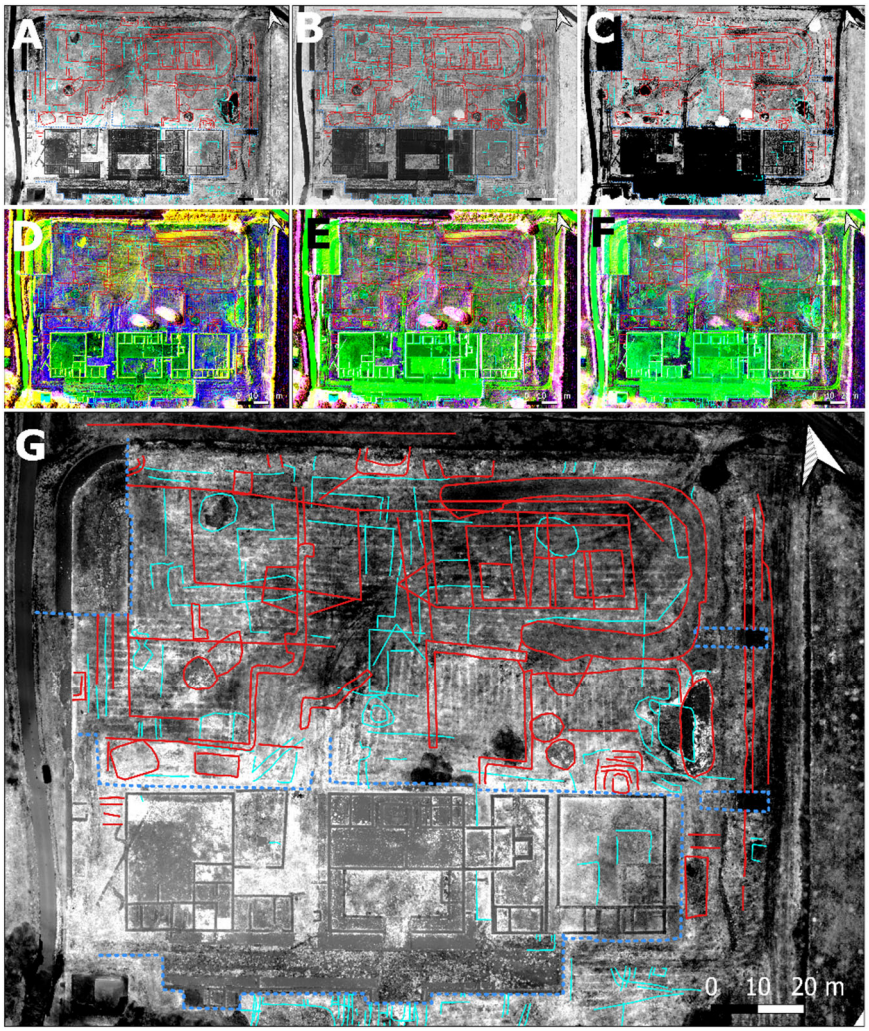


Figure 12. (**A**) NDVI June 2022. (**B**) NDVI October 2022. (**C**) NDVI March 2023. (**D**) PCA October 2022–March 2023. (**E**) PCA June 2022–October 2022. (**F**) PCA June 2022–March 2023. (**G**) NDVI Difference October 2022–March 2023.

Among the detected crop marks, one in the shape of a 'U' is particularly notable (Figure 13), indicated in green in the figure. It is in the northeast of the site and is known to have been caused by the earth mounds (terreras) from the 1934 excavation directed by S. González and Á. del Castillo, which were removed during the 2009 excavation and consolidation campaign [44]. It is important to note that the variability in vegetation appears to have facilitated the detection of this crop mark. There is a predominance of shrub species and moss (Figure 13D) in the crop mark area, compared to the predominance of herbaceous species (Figure 13E) in the area adjacent to the crop mark.

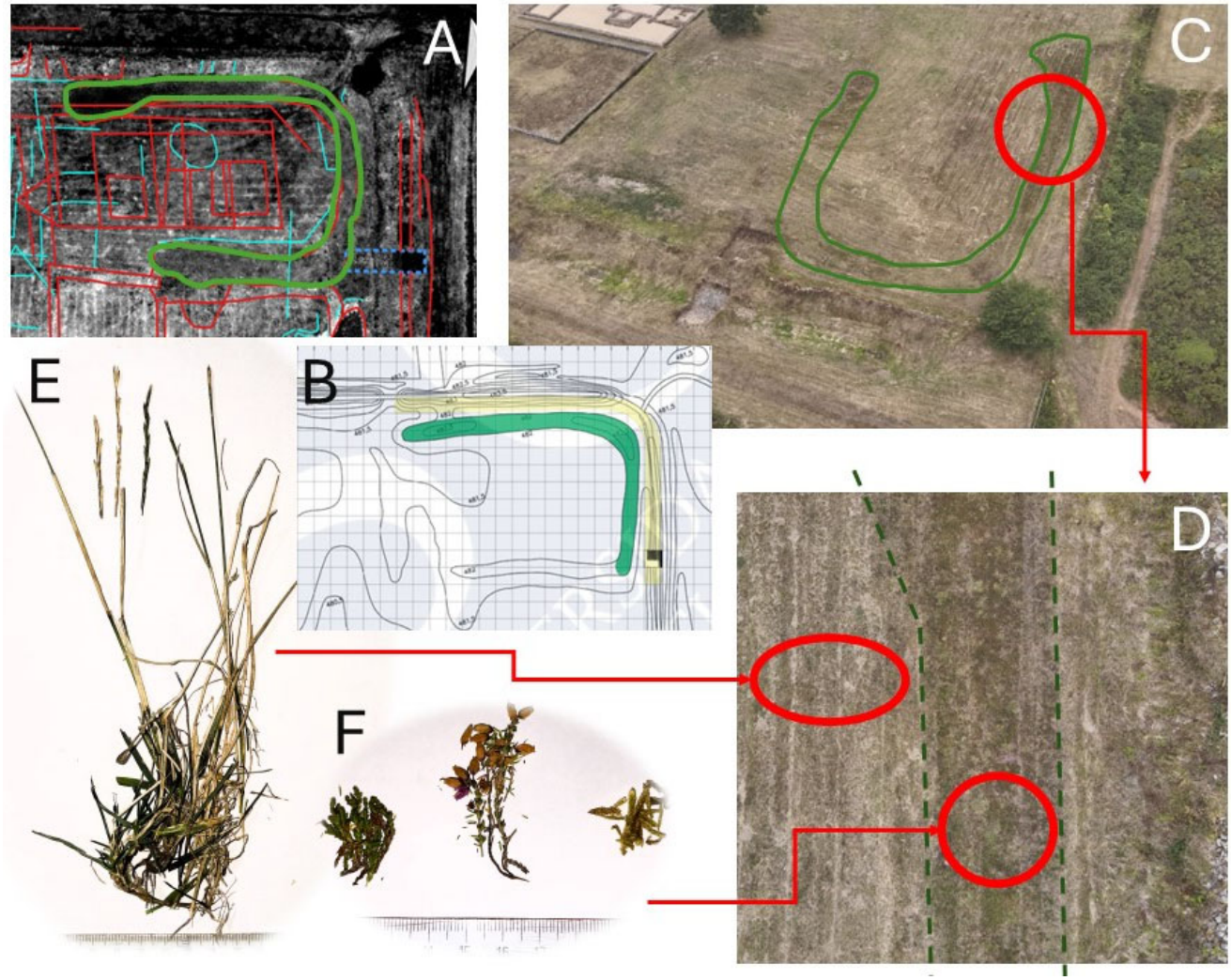


Figure 13. Case 4, A Cidadela, Sobrado dos Monxes. (**A**) NDVI Difference October 2022–March 2023. (**B**) Graphic documentation by Costa-García 2013. (**C**) Aerial photograph. (**D**) Detailed photograph. (**E**) Area with predominance of herbaceous species. (**F**) Area with predominance of small shrub species and moss.

Thus, the surface heterogeneity, which was initially considered a disadvantage compared to monoculture areas, could be advantageous in this study context.

3.2.5. Case 5

In this case study, three multispectral flights were conducted. Figure 14A shows the RGB orthomosaic of the study area from the multispectral flight conducted in September 2021. Figure 14B displays the color infrared (521) composition from the same flight. In this case study, some structures were detected in an area of heterogeneous grassland, which presumably correspond to circular Iron Age dwellings, as the dimensions of excavated dwellings nearby match the detected marks.

Figure 15A–C show the crop marks detected in Case 4, overlaid on the true color orthomosaics corresponding to the three flight dates over the area. Figure 15D–F present the vectorized crop marks over the NDVI indices. In red, the most evident marks vectorized using the NDVI index set can be observed. In cyan, less evident marks vectorized using other indices or color compositions are shown.

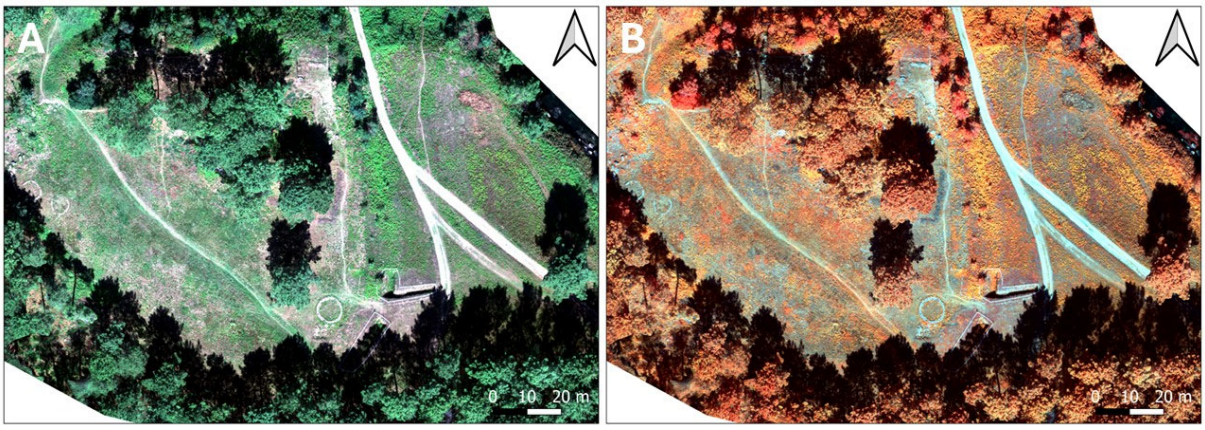


Figure 14. September 2021 Flight. (**A**) RGB; (**B**) Color Infrared (521). The arrow indicates north.

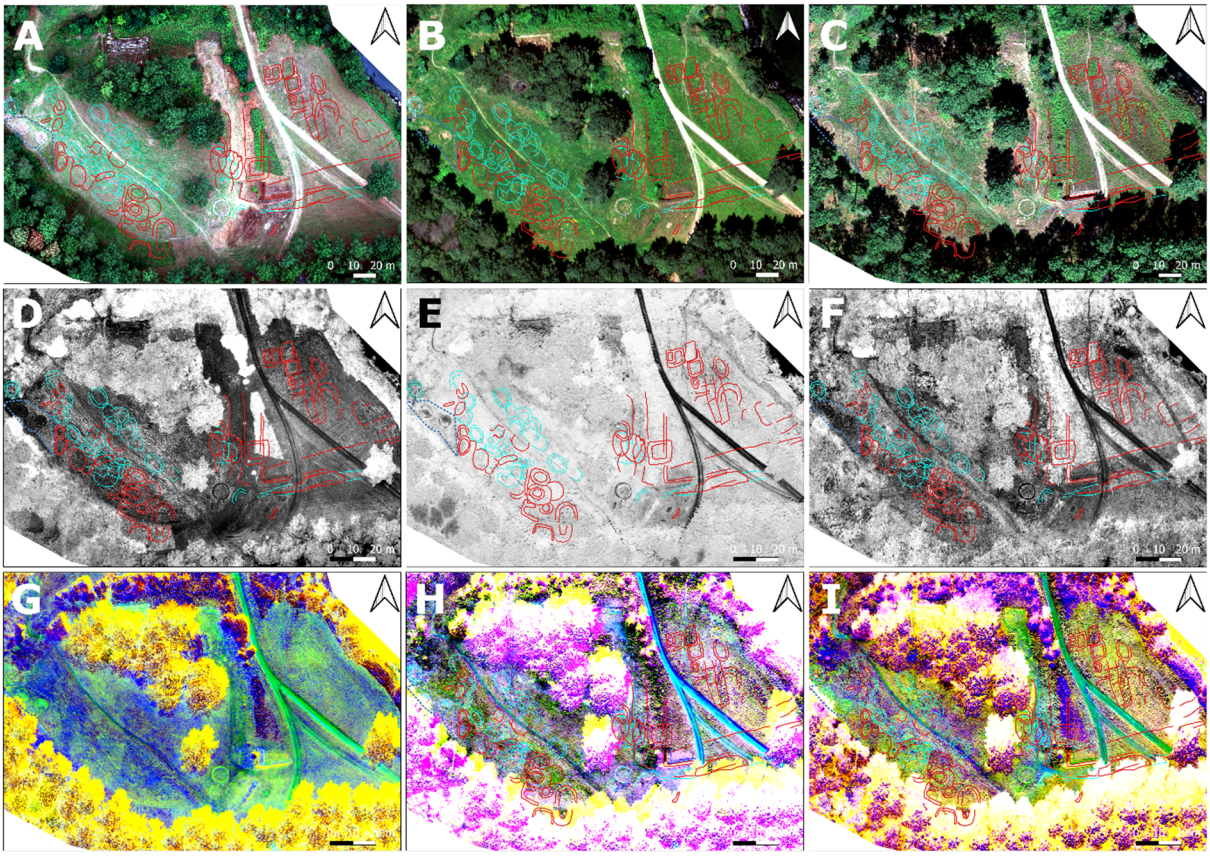


Figure 15. (**A**) RGB September 2021; (**B**) RGB May 2022; (**C**) RGB September 2022; (**D**) NDVI September 2021; (**E**) NDVI May 2022; (**F**) NDVI September 2022; (**G**) PCA September 2021–May 2022; (**H**) PCA May 2022–September 2022; (**I**) PCA September 2021–September 2022. The arrow indicates north.

Among the three multispectral flights conducted at this site—September 2021, May 2022, and September 2022—the September 2021 flight, conducted after a dry summer, provides the best results for detecting crop marks. The May 2022 flight, in mid-spring, shows the least amount of crop marks. However, the September 2022 flight, following another dry summer, yields good results again. The coloured compositions from the PCA analyses, when combined in pairs, highlight numerous potential crop marks that suggest a possible correlation with buried structures, as shown in Figure 15G–I. Nevertheless, further excavation would be necessary to confirm this hypothesis.

3.2.6. Case 6

In this case study, three multispectral flights were conducted: in the summer of 2022 and in the winter and spring of 2023. Figure 16A presents the false color composition 123 from August 2022, while Figure 16C,E show the RGB orthomosaics from February and April 2023, respectively. Figure 16B,D,F correspond to the NDVI indices for the same periods. The site features two clearly distinct areas: one of grassland and the other of scrubland, the latter having been affected by a fire prior to data acquisition. The results reveal the presence of crop marks in both areas, which could potentially correspond to castro-style dwellings or defensive structures. In the grassland area, the flight conducted during the dry summer of 2022 provides the best results for detecting crop marks. Conversely, the flight in May 2022, during mid-spring, shows the least prominent crop marks. In red, the most evident marks, mostly extracted from the NDVI index, are shown. In cyan, less evident marks extracted from other indices or compositions are displayed.

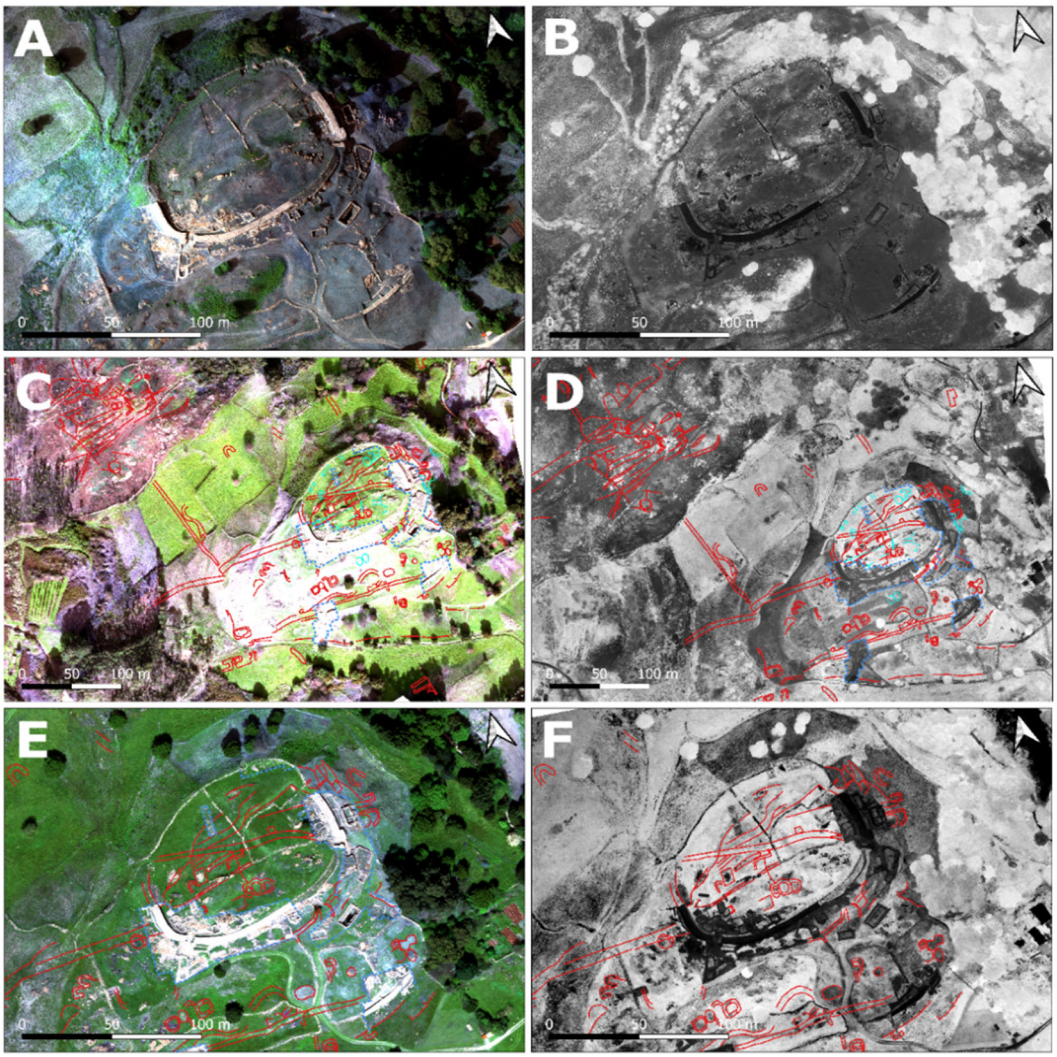


Figure 16. Orthomosaics in Case 6. (**A**) Composition 123, August 2022 (**B**) NDVI August 2022 (**C**) RGB February 2023 (**D**) NDVI February 2023 (**E**) RGB April 2023 (**F**) NDVI April 2023. The arrow indicates north.

It is worth noting that a "banding" effect is observed, particularly in the false color composition 123 from August 2022, as shown in Figure 16A. This phenomenon refers to the appearance of visible bands in the images due to variations in radiometry during image capture. Vegetation indices, such as NDVI, largely corrected these defects, allowing for a

more accurate analysis. In this case, the banding issue is exacerbated by the dark, nearly black tone in the area affected by the fire, which contrasts with the adjacent areas that maintain their usual radiometry. This contrast complicates the adjustment of exposure parameters during image capture. Although radiometric calibration before generating the orthomosaic mitigates this effect, it does not completely eliminate it. This problem is present in various case studies, being particularly noticeable in this one.

In the post-fire regeneration area, the crop marks are most clearly visible during the last flight in May 2023, the following spring after the summer fire, compared to the flights from August 2022, just weeks after the fire, and February 2023, still in winter. As shown in Figure 17, the results suggest that this context favours the identification of crop marks. However, there is no clear certainty regarding their relation to buried structures without conducting excavations to confirm it.

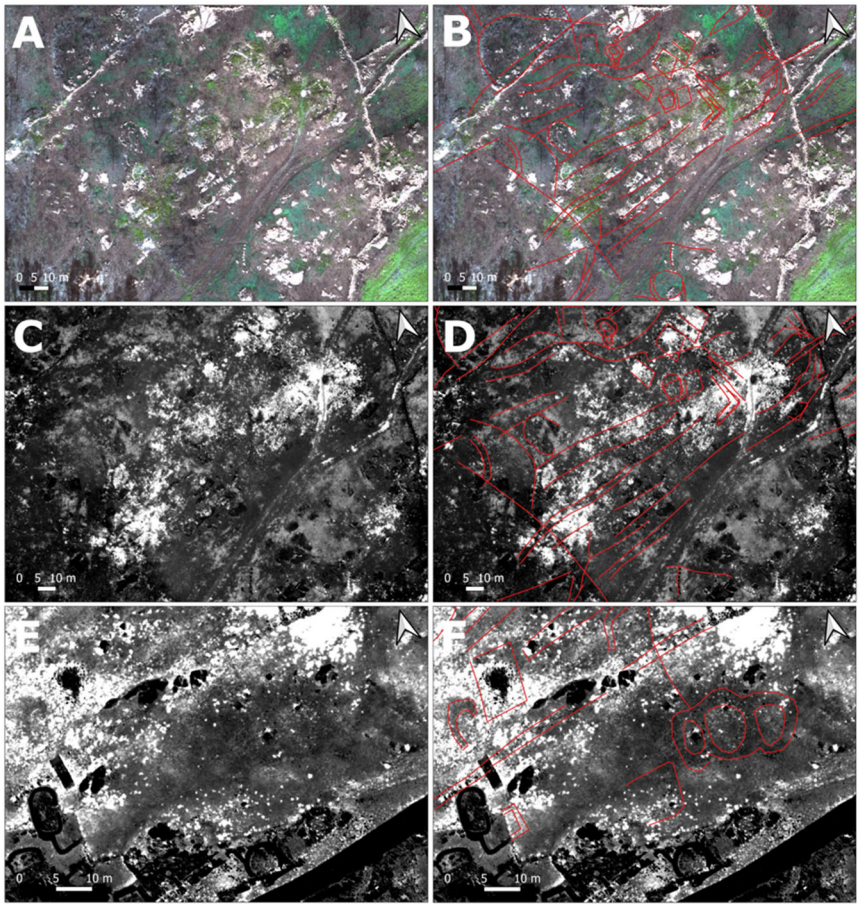


Figure 17. Orthomosaics of the post-fire regeneration area. (**A**) RGB May 2023 (**B**) Crop Mark on RGB. (**C**) NDVI May 2023 (**D**) Crop Mark on NDVI. (**E**) NDVI May 2023 (second area) (**F**) Crop Mark on NDV (second area). The arrow indicates north.

4. Discussion

The analyses conducted across the six case studies demonstrate the effectiveness of multispectral imagery and vegetation indices, such as NDVI, for the preliminary identification of crop marks and buried archaeological structures. PCA of individual or combined flights has proven particularly valuable in highlighting areas of interest, enabling differentiation between ancient structures, such as walls and ditches associated with fortified settlements, and modern terrain alterations, such as those caused by agricultural machinery or previous excavations. It is important to note that the results of vectorization are merely examples of potential crop marks, as they were carried out by technicians who are not experts in heritage. Therefore, these results should be validated in the future through

excavations in the study areas. Furthermore, it is essential to recognize that a rigorous application of this technique requires a multidisciplinary team or experts with specialized knowledge in the field of heritage.

Cases involving multiple flights indicate that summer, when vegetation is more stressed, is the optimal time for detecting crop marks in grasslands. In contrast, in scrubland or post-fire regeneration areas, detection is more effective during the peak growing season in spring.

It is noteworthy that vegetation variability has proven advantageous in detecting crop marks across different case studies. Natural vegetation aids in locating these marks, as plant species tend to distribute themselves according to the underlying terrain characteristics. Initially, the heterogeneity of the surface was considered a disadvantage compared to studies in monoculture areas, but results suggest that this heterogeneity could offer significant benefits in detecting and analysing potential archaeological features. Furthermore, planning maintenance work in the study area could facilitate the use of these techniques, improving conditions for detecting crop marks and other archaeological signals.

Regarding the visible spectrum, the false color composition 123 has generally yielded better results than the true color composition 321 for detecting crop marks, indicating an effective application of the technique with RGB sensors. It is important to note that, in this case, the composition was created using individual sensors for each band.

The observation of banding effects in several cases suggests that the use of automatic settings in photographic recording is a variable that should be reconsidered. Flight planning applications default to automatic mode; however, results suggest exploring alternative flight strategies, including pre-flight parameter adjustments and manual settings.

5. Conclusions

This study highlights the potential of UAS-captured imagery and image processing techniques for detecting and mapping archaeological sites in heterogeneous agricultural environments. The decreasing costs associated with capturing multispectral images using UAS, coupled with their high spatial and temporal resolution, enable researchers to advance the understanding of the distribution and nature of ancient settlements, such as the fortified hillforts of northwest Iberia, without resorting to invasive methods that could damage archaeological sites.

Several case studies clearly demonstrate the relationship between identified crop marks and semi-excavated archaeological structures, including smaller walls that constitute the hillfort dwellings. This confirms the usefulness of these non-invasive methods for archaeological prospecting in such environments. However, interpreting crop marks has been particularly challenged by recent disturbances to the terrain and, to a lesser extent, by factors such as climatic variability, which in some cases has complicated the clear identification of buried structures, as anticipated in prior literature. While this methodology does not provide as conclusive results as other non-invasive subsurface techniques, such as ground-penetrating radar, it has proven capable of detecting remains under favourable conditions. Notably, this methodology's ability to detect historical excavations is of particular interest, given that past georeferencing methods were incomplete and imprecise. This approach has proven more agile in locating these interventions, facilitating the resolution of issues related to documenting and locating past interventions.

Despite the mentioned limitations, the results indicate that the remote sensing techniques employed provide valuable insights into the location of potentially buried, unexplored structures, underscoring their potential as a non-invasive technique to guide archaeological excavation planning. The accessibility of these technologies—whether through direct operation of a multispectral UAS by heritage professionals or through the democratization of these services—allows the described methodology to be applied for obtaining information on crop marks before planning an intervention. This could significantly transform how archaeological research is approached in the future.

Supplementary Materials: The following supporting information can be downloaded at: https://www.mdpi.com/article/10.3390/rs16213923/s1, File S1: reportcase1. File S2: reportcase2; File S3: reportcase3; File S4: reportcase4; File S5: reportcase5; File S6: reportcase6.

Author Contributions: Conceptualization, methodology, writing—original draft, S.P.-V.; investigation, visualization and software, J.O.-S.; project administration, funding acquisition, writing—review, formal analysis and editing, M.G.-D. All authors have read and agreed to the published version of the manuscript.

Funding: This research was funded by the European Commission, through the INTERREG POCTEP (Spain–Portugal) Programme, grant number 0054_AEROGANP_1_E and by Xunta de Galicia through the aids for consolidation and structuring of competitive research units in the universities of the Galician University System 2023_2025, grant number ED431B 2023/17.

Data Availability Statement: Data are contained within the article and Supplementary Materials.

Conflicts of Interest: The authors declare no conflicts of interest.

References

1. Crawford, O.G.S. Woodbury. Two Marvellous Air–Photographs. *Antiquity* **1929**, *3*, 452–455. [CrossRef]
2. Neogrády, S. A Légifénykép És Az Archeológiai Kutatások. *Térképészeti Közlöny* **1950**, *7*, 283–332.
3. Masini, N.; Marzo, C.; Manzari, P.; Belmonte, A.; Sabia, C.; Lasaponara, R. On the characterization of temporal and spatial patterns of archaeological crop-marks. *J. Cult. Herit.* **2018**, *32*, 124–132. [CrossRef]
4. Czajlik, Z.; Árvai, M.; Mészáros, J.; Nagy, B.; Rupnik, L.; Pásztor, L. Cropmarks in Aerial Archaeology: New Lessons from an Old Story. *Remote Sens.* **2021**, *13*, 1126. [CrossRef]
5. Verhoeven, G.J. Near-Infrared Aerial Crop Mark Archaeology: From its Historical Use to Current Digital Implementations. *J. Archaeol. Method Theory* **2012**, *19*, 132–160. [CrossRef]
6. Cavalli, R.M.; Colosi, F.; Palombo, A.; Pignatti, S.; Poscolieri, M. Remote hyperspectral imagery as a support to archaeological prospection. *J. Cult. Herit.* **2007**, *8*, 272–283. [CrossRef]
7. Rowlands, A.; Sarris, A. Detection of exposed and subsurface archaeological remains using multi-sensor remote sensing. *J. Archaeol. Sci.* **2007**, *34*, 795–803. [CrossRef]
8. Beck, A.; Cowley, D.C. Archaeological Applications of Multi/Hyper-Spectral Data–Challenges and Potential. In *Remote Sensing for Archaeological Heritage Management*; Europae Archaeologia Consilium: Budapest, Hungary, 2011; pp. 87–97.
9. Doneus, M.; Verhoeven, G.; Atzberger, C.; Wess, M.; Ruš, M. New ways to extract archaeological information from hyperspectral pixels. *J. Archaeol. Sci.* **2014**, *52*, 84–96. [CrossRef]
10. Atzberger, C.; Wess, M.; Doneus, M.; Verhoeven, G. ARCTIS—A MATLAB® Toolbox for Archaeological Imaging Spectroscopy. *Remote Sens.* **2014**, *6*, 8617–8638. [CrossRef]
11. Duarte, L.; Sánchez, J.G.; Fonte, J.; Teodoro, A.C. A GIS Open-Source Application to Enhance the Identification of Archaeological Crop Marks Using Remote Sensing Data. In Proceedings of the Earth Resources and Environmental Remote Sensing/GIS Applications XII, Online, 13–18 September 2021; Volume 11863, pp. 91–99.
12. Verhoeven, G.; Vermeulen, F. Engaging with the Canopy—Multi-Dimensional Vegetation Mark Visualisation Using Archived Aerial Images. *Remote Sens.* **2016**, *8*, 752. [CrossRef]
13. Kaimaris, D. Utilization of Different Sensors in UAV for the Detection and Optimal Visual Observation of the Marks over Buried Ancient Remains. *Sci. Cult.* **2022**, *8*, 129–145. [CrossRef]
14. Agapiou, A.; Hadjimitsis, D.G.; Alexakis, D.D. Evaluation of Broadband and Narrowband Vegetation Indices for the Identification of Archaeological Crop Marks. *Remote Sens.* **2012**, *4*, 3892–3919. [CrossRef]
15. Fuldain González, J.J.; Varón Hernández, F.R. NDVI Identification and Survey of a Roman Road in the Northern Spanish Province of Álava. *Remote Sens.* **2019**, *11*, 725. [CrossRef]
16. Aqdus, S.A.; Hanson, W.S.; Drummond, J. The potential of hyperspectral and multi-spectral imagery to enhance archaeological cropmark detection: A comparative study. *J. Archaeol. Sci.* **2012**, *39*, 1915–1924. [CrossRef]
17. Lehmann, J.R.K.; Smithson, K.Z.; Prinz, T. Making the Invisible Visible: Using UAS-Based High-Resolution Color-Infrared Imagery to Identify Buried Medieval Monastery Walls. *J. Unmanned Veh. Syst.* **2015**, *3*, 58–67. [CrossRef]
18. Ortiz, J.; Gil, M.L.; Martínez, S.; Rego, T.; Meijide, G. Three-dimensional Modelling of Archaeological Sites Using Close-range Automatic Correlation Photogrammetry and Low-altitude Imagery. *Archaeol. Prospect.* **2013**, *20*, 205–217. [CrossRef]
19. Remondino, F.; Barazzetti, L.; Nex, F.; Scaioni, M.; Sarazzi, D. UAV photogrammetry for mapping and 3D modeling–current status and future perspectives. International Archives of the Photogrammetry. *Remote Sens. Spat. Inf. Sci.* **2011**, *38*, C22.
20. Themistocleous, K.; Ioannides, M.; Agapiou, A.; Hadjimitsis, D.G. The Methodology of Documenting Cultural Heritage Sites Using Photogrammetry, UAV, and 3D Printing Techniques: The Case Study of Asinou Church in Cyprus. In Proceedings of the Third International Conference on Remote Sensing and Geoinformation of the Environment (RSCy2015), Paphos, Cyprus, 16–19 March 2015; Volume 9535, pp. 312–318.

21. Themistocleous, K. Themistocleous, K. The Use of UAVs for Cultural Heritage and Archaeology. In *Remote Sensing for Archaeology and Cultural Landscapes*; Springer: Berlin/Heidelberg, Germany, 2020; pp. 241–269.
22. Stek, T.D. Drones over Mediterranean Landscapes. The Potential of Small UAV's (Drones) for Site Detection and Heritage Management in Archaeological Survey Projects: A Case Study from Le Pianelle in the Tappino Valley, Molise (Italy). *J. Cult. Herit.* **2016**, *22*, 1066–1071. [CrossRef]
23. Campana, S. Drones in Archaeology. State-of-the-art and Future Perspectives. *Archaeol. Prospect.* **2017**, *24*, 275–296. [CrossRef]
24. Gil-Docampo, M.; Peña-Villasenín, S.; Bettencourt, A.M.S.; Ortiz-Sanz, J.; Peraleda-Vázquez, S. 3D geometric survey of cultural heritage by UAV in inaccessible coastal or shallow aquatic environments. *Archaeol. Prospect.* 2023, *early view*. [CrossRef]
25. Moriarty, C.; Cowley, D.C.; Wade, T.; Nichol, C.J. Deploying Multispectral Remote Sensing for Multi-temporal Analysis of Archaeological Crop Stress at Ravenshall, Fife, Scotland. *Archaeol. Prospect.* **2019**, *26*, 33–46. [CrossRef]
26. Hill, A.C.; Laugier, E.J.; Casana, J. Archaeological Remote Sensing Using Multi-Temporal, Drone-Acquired Thermal and Near Infrared (NIR) Imagery: A Case Study at the Enfield Shaker Village, New Hampshire. *Remote Sens.* **2020**, *12*, 690. [CrossRef]
27. Opitz, R.; Herrmann, J. Recent Trends and Long-standing Problems in Archaeological Remote Sensing. *J. Comput. Appl. Archaeol.* **2018**, *1*, 19–41. [CrossRef]
28. Lasaponara, R.; Masini, N. *Satellite Remote Sensing: A New Tool for Archaeology*; Springer: Berlin/Heidelberg, Germany, 2012; Volume 16.
29. Luo, L.; Wang, X.; Guo, H.; Lasaponara, R.; Zong, X.; Masini, N.; Wang, G.; Shi, P.; Khatteli, H.; Chen, F.; et al. Airborne and spaceborne remote sensing for archaeological and cultural heritage applications: A review of the century (1907–2017). *Remote Sens. Environ.* **2019**, *232*, 111280. [CrossRef]
30. Evans, R.; Jones, R. Crop marks and soils at two archaeological sites in Britain. *J. Archaeol. Sci.* **1977**, *4*, 63–76. [CrossRef]
31. Hejcman, M.; Smrž, Z. Cropmarks in stands of cereals, legumes and winter rape indicate sub-soil archaeological features in the agricultural landscape of Central Europe. *Agric. Ecosyst. Environ.* **2010**, *138*, 348–354. [CrossRef]
32. Wilson, D.R. Reading the palimpsest: Landscape studies and air-photography. *Landsc. Hist.* **1987**, *9*, 5–25. [CrossRef]
33. Doneus, M. *Die Hinterlassene Landschaft-Prospektion Und Interpretation in Der Landschaftsarchäologie*; Verlag der Österreichischen Akademie der Wissenschaften: Wien, Austria, 2013; Volume 78.
34. Parcak, S.H. *Satellite Remote Sensing for Archaeology*; Routledge: London, UK, 2009.
35. Kaimaris, D.; Patias, P. Systematic Observation of the Change of Marks of Known Buried Archaeological Structures: Case study in the Plain of Philippi, Eastern Macedonia, Greece. *Mediterr. Archaeol. Archaeom.* **2015**, *15*, 129.
36. Kaimaris, D.; Patias, P.; Tsakiri, M. Best period for high spatial resolution satellite images for the detection of marks of buried structures. *Egypt. J. Remote Sens. Space Sci.* **2012**, *15*, 9–18. [CrossRef]
37. Agapiou, A.; Hadjimitsis, D.G.; Sarris, A.; Georgopoulos, A.; Alexakis, D.D. Optimum temporal and spectral window for monitoring crop marks over archaeological remains in the Mediterranean region. *J. Archaeol. Sci.* **2013**, *40*, 1479–1492. [CrossRef]
38. Braasch, O. Vom Heiteren Himmel. In *Luftbildar Chäologie. (Por Trät Archäologie 1)*; Gesellschaft Für Vor und Frühgeschichte in Württemberg und Hohenzollern: Esslingen, Germany, 2005.
39. Ahmed, O.S.; Shemrock, A.; Chabot, D.; Dillon, C.; Williams, G.; Wasson, R.; Franklin, S.E. Hierarchical land cover and vegetation classification using multispectral data acquired from an unmanned aerial vehicle. *Int. J. Remote Sens.* **2017**, *38*, 2037–2052. [CrossRef]
40. Mesas-Carrascosa, F.J.; Rumbao, I.C.; Torres-Sánchez, J.; García-Ferrer, A.; Peña, J.M.; Granados, F.L. Accurate ortho-mosaicked six-band multispectral UAV images as affected by mission planning for precision agriculture proposes. *Int. J. Remote Sens.* **2017**, *38*, 2161–2176. [CrossRef]
41. El Imanni, H.S.; El Harti, A.; Bachaoui, E.M.; Mouncif, H.; Eddassouqui, F.; Hasnai, M.A.; Zinelabidine, M.I. Multispectral UAV data for detection of weeds in a citrus farm using machine learning and Google Earth Engine: Case study of Morocco. *Remote Sens. Appl. Soc. Environ.* **2023**, *30*, 100941. [CrossRef]
42. Kaimaris, D.; Tsokas, D. Application of UAS with Remote Sensing Sensors for the Location of Marks in the Archaeological Site of the Europos, Greece. *Remote Sens.* **2023**, *15*, 3843. [CrossRef]
43. Sakamoto, T.; Ogawa, D.; Hiura, S.; Iwasaki, N. Alternative Procedure to Improve the Positioning Accuracy of Orthomosaic Images Acquired with Agisoft Metashape and DJI P4 Multispectral for Crop Growth Observation. *Photogramm. Eng. Remote Sens.* **2022**, *88*, 323–332. [CrossRef]
44. Costa-García, J.M. Las Primeras Intervenciones Arqueológicas En A Cidadela (Sobrado Dos Monxes, A Coruña). *Gallaecia Rev. Arqueol. Antigüidade* **2013**, *32*, 109–127. [CrossRef]

Disclaimer/Publisher's Note: The statements, opinions and data contained in all publications are solely those of the individual author(s) and contributor(s) and not of MDPI and/or the editor(s). MDPI and/or the editor(s) disclaim responsibility for any injury to people or property resulting from any ideas, methods, instructions or products referred to in the content.